



Published in final edited form as:

Angew Chem Int Ed Engl. 2021 February 15; 60(7): 3603–3610. doi:10.1002/anie.202005934.

Glycoengineering of NK cells with glycan ligands of CD22 and selectins for B-cell lymphoma therapy

Senlian Hong^[a], Chenhua Yu^{[a],[b]}, Peng Wang^[a], Yujie Shi^[a], Weiqian Cao^[c], Bo Cheng^[d], Digantkumar G. Chapla^[e], Yuanhui Ma^[a], Jie Li^[a], Emily Rodrigues^[f], Yoshiki Narimatsu^[g], John R. Yates III^[a], Xing Chen^[d], Henrik Clausen^[g], Kelly W. Moremen^[e], Matthew Scott Macauley^[f], James C. Paulson^[a], Peng Wu^[a]

^[a]Department of Molecular Medicine, The Scripps Research Institute, La Jolla, California, 92037, U.S.A.

^[b]Tianjin Medical University Cancer Institute & Hospital, Key laboratory of Breast Cancer Prevention and Therapy; School of Medicine, Nankai University, Tianjin 300071, China

^[c]Department of Chemistry and Institutes of Biomedical Sciences, The Fifth People's Hospital, Fudan University, Shanghai 200433, China

^[d]College of Chemistry and Molecular Engineering, Beijing University, Beijing 100871, China

^[e]Complex Carbohydrate Research Center, University of Georgia, Athens, Georgia, 30602, U.S.A.

^[f]Department of Chemistry, University of Alberta, 11227 Saskatchewan Dr NW, Edmonton, AB T6G 2G2, Alberta, Canada

^[g]Copenhagen Center for Glycomics, Department of Cellular and Molecular Medicine, University of Copenhagen, Copenhagen, Denmark

Abstract

CD22, a member of Siglec family of sialic acid binding proteins, has restricted expression on B cells. Antibody-based agents targeting CD22 or CD20 on B lymphoma and leukemia cells exhibit clinical efficacy for treating these malignancies, but also attack normal B cells leading to immune deficiency. Here, we report a chemoenzymatic glycocalyx editing strategy to introduce high-affinity and specific CD22 ligands onto NK-92MI and cytokine-induced killer cells to achieve tumor-specific CD22 targeting. These CD22-ligand modified cells exhibited significantly enhanced tumor cell binding and killing *in vitro* without harming healthy B cells. For effective lymphoma cell killing *in vivo* we further functionalized CD22 ligand-modified NK-92MI cells with the E-selectin ligand sialyl Lewis X to promote trafficking to bone marrow. The dual-functionalized cells resulted in the efficient suppression of B lymphoma in a xenograft model. Our results suggest that nature killer cells modified with glycan ligands to CD22 and selectins promote both targeted killing of B lymphoma cells and improved trafficking to sites where the cancer cells reside, respectively.

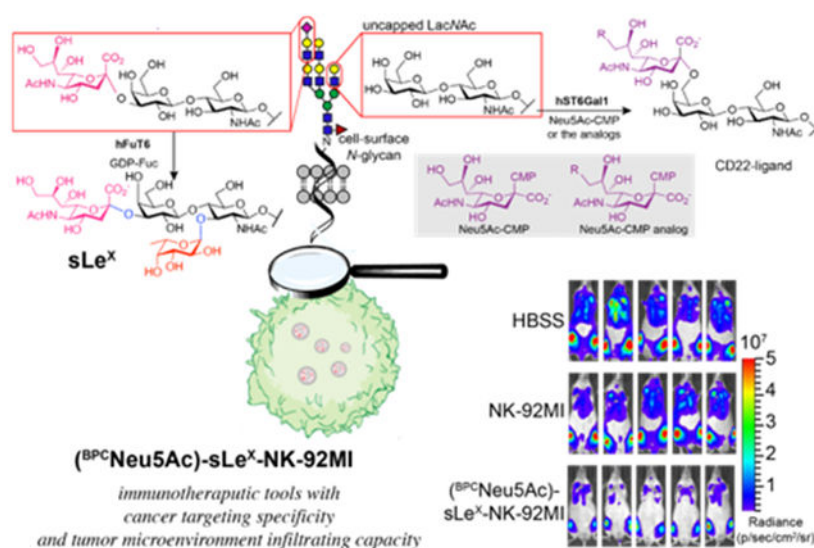
S.H. (senlian@scripps.edu), J.C.P.(jpaulson@scripps.edu), P.W. (pengwu@scripps.edu).

Supporting information for this article is given via a link at the end of the document.

Graphical Abstract

Exploring the exogenous glycotransferase-assisted chemoenzymatic approaches to edit the structure of live immune cell-surface glycans, in turn, enables in situ generation of the ligands for cancer specific pathology-markers. Here we reported the creation of CD22-specific ligands and sialyl Lewis X on NK cells (NK-92MI or CIK cells) to target and eradicate B-lymphoma efficiently.

Glycoengineering, a way to efficiently target cell-therapeutics to tumor sites



Keywords

CD22 ligand; chemoenzymatic glycan editing; B-lymphoma cancer; sLeX; E-selectin

Introduction

Current treatments for patients with B cell malignancies, such as non-Hodgkin lymphoma and leukemia primarily rely on systemic chemotherapy and the anti-CD20 antibody rituximab. However, when people become resistant to both, new treatments are needed.^[1,2] CD22, also known as sialic acid-binding immunoglobulin-like lectin 2 (Siglec-2), is a B cell restricted inhibitory receptor for antagonizing B cell receptor signaling. CD22 is highly expressed by various B lymphoma and leukemia.^[3,4] Its B cell restricted expression and endocytic nature make CD22 a promising therapeutic target. CD22-specific antibodies and antibody-drug conjugate-based therapies have shown clinical efficacies to treat aggressive and follicular non-Hodgkin's lymphoma, acute lymphoblastic leukemia and diffuse large B cell lymphoma.^[5] However, these agents cannot differentiate healthy B cells from B malignancies and cause serious side effects such as low blood counts, systemic cytotoxic effects and veno-occlusive disease (VOD). Recently, Fry and co-workers reported that anti-CD22 engineered Chimeric antigen receptor T cells (anti-CD22 CAR-Ts) induced similar response rates as anti-CD19 CAR-T cells in patients with acute lymphoblastic leukemia.^[6-9] However, CAR-T therapies face the same dilemma of on-target-off-tumor toxicity.

Unnatural sialic acid analogs with high-affinity and specificity for CD22 are promising surrogates of antibodies for CD22 targeting.^[10-14] By introducing unnatural substituents onto C9 of Neu5Ac, sialic acid analogs with micromolar affinity for CD22 have been discovered, such as 9-*N*-biphenylcarboxamide-Neu5Ac (^{BPC}Neu5Ac^[10]; **1**) and 9-*N*-*m*-phenoxybenzamide-Neu5Ac (^{MPB}Neu5Ac^[12]; **2**). Nanoparticles that display these ligands multivalently have been used to deliver cytotoxic drugs to CD22 over-expressed tumor cells in animal models.^[15-17] Like antibody-based reagents, nanoparticles equipped with CD22 ligands target all cells expressing CD22. To employ CD22 targeting ligands to channel cytotoxic agents for tumor-specific killing, the challenge is to decouple the killing mechanism from CD22 targeting.

NK-92MI is a non-immunogenic and constantly cytotoxic nature killer (NK) cell line currently undergoing intensive clinical trials as an “off-the-shelf therapeutics” for treating both hematological and solid malignancies.^[18-20] NK-92MI-induced killing relies on the interaction of NK activation receptors, e.g. NKG2D, with their ligands that have restricted expressions on stressed and malignant cells, and thus systemic toxicity is eliminated.^[20] However, NK-92MI cells lack tumor-specific targeting capabilities, and as a consequence they only exhibit weak to negligible tumor-control effects when administered *in vivo*.^[21,22] Like NK-92MI cells, cytokine-Induced Killer (CIK) cells that feature a mixed T- and NK cell-like phenotype^[23-26] mainly rely on NKG2D to induce tumor cell killing.^[26] We hypothesize that by using NK-92MI and CIK cells functionalized with high-affinity and CD22-specific ligands, selective targeting and killing of tumor cells with CD22 over-expression can be achieved.^[27,28]

Here, we exploit chemoenzymatic glycan editing^[29] to create high-affinity CD22 ligands on the cell surface of NK-92MI and CIK cells. We demonstrate that the functionalized NK-92MI and CIK cells display high-affinity CD22 ligands on their *N*-glycans and form multivalent ligand presentation, which leads to significantly enhanced binding and killing of CD22 over-expressed tumor cells *in vitro* while leaving healthy B cells untouched. *In vivo* in a xenograft lymphoma model, however, the functionalized NK-92MI cells only show weak activities. In this model, E-selectin that is constitutively expressed in the bone marrow binds to lymphoma cells, facilitates their bone-marrow deposition, and shed them from attacking by NK-92MI cells. We discovered that NK-92MI cells that are functionalized with CD22 ligands can be further engineered via fucosyltransferase-mediated installation of E-selectin ligands to enhance their bone marrow migration. In this way, significant suppression of B-lymphoma proliferation *in vivo* is achieved.

Results

Engineering CD22 ligands on live cells via chemoenzymatic glycan editing.

To engineer killer cells for targeting CD22 positive tumors, we sought to install CD22 ligands onto their cell surfaces directly. Because the sialylated epitope Neu5Ac α 2-6Gal β 1-4GlcNAc found at peripheral *N*-glycans is a natural ligand of CD22,^[14] we first evaluated the possibility of employing sialyltransferase (ST)-mediated glycan editing to create this epitope on mammalian cell surfaces by using Chinese hamster ovary (CHO) Lec2 mutant cells^[30,31] and an engineered HEK293 cell line³² (HEK293- ST), a

human epithelial cell line with inactivated ST6Gal1/2 and ST3Gal3/4/6 sialyltransferase genes and selective loss of sialic acids on *N*-glycans and glycolipids but not on some types of O-glycans, as model systems. Both cell lines possess complex type *N*-glycans terminated with *N*-acetylglucosamine (type 2 LacNAc Gal β 1-4GlcNAc, or in the case of HEK293 also minor amounts of LacDiNAc, GalNAc β 1-4GlcNAc) as is the case for most mammalian cells. Two α 2-6STs, the truncated human ST6Gal1^[33] and *Photobacterium damsela* 2,6ST (Pd2,6ST^[34,35]), were evaluated for this endeavor using biotinylated CMP-Neu5Ac^[36] as the donor. Approximately 2fold more biotin-Neu5Ac was incorporated onto Lec2 cells by ST6Gal1 compared to that added by Pd2,6ST (Supplementary figure s1). Therefore, ST6Gal1 was chosen for the follow-up cell-surface glycan engineering experiment (Figure 1a).

Incubating Lec2 and HEK293- ST cells with ST6Gal1 in the presence of CMP-Neu5Ac resulted in robust CD22-Fc binding, whereas the cells treated with ST3Gal4^[37,38] and CMP-Neu5Ac to create Neu5Ac α 2-3Gal β 1-4GlcNAc on the surface only exhibited background signals (Figure 1b and c and Supplementary figure s3a). As revealed by matrix-assisted laser desorption/ionization time-of-flight mass spectrometer (MALDI-TOF), after ST6Gal1 mediated sialylation, sialylated di-, tri-, and tetra-branched *N*-glycans could be detected on the modified HEK293- ST cells (Supplementary figure s4). Interestingly, under saturated conditions a comparable level of newly added-Neu5Ac on Lec2 and HEK293- ST cells (Supplementary figure s5) led to a 1.5fold higher CD22-Fc binding on HEK293- ST cells than on Lec2 cells (Figure 1d).

Two unnatural Neu5Ac analogs, ^{BPC}Neu5Ac (**2a**) and ^{MPB}Neu5Ac (**2b**), when α 2-6-linked to LacNAc, are known to bind to CD22 with affinities in the submicromolar range.^[12] We then assessed the feasibility of using the corresponding CMP sugars of these two analogs as the donor substrates for ST6Gal1-assisted sialylation to generate high-affinity CD22 ligands on the cell surface (Figure 2a, Supplementary figure s17, and s18). At all donor concentrations assessed, Lec2 cells (Figure 2b and Supplementary figure s6a) and HEK293- ST cells (Supplementary figure 65b-d) that were modified with unnatural substrates showed significantly higher binding to CD22-Fc binding than the cells treated with CMP-Neu5Ac. Under saturating conditions, approximately 10-fold and 500-fold higher CD22 binding was detected on CMP-^{BPC}Neu5Ac- and CMP-^{MPB}Neu5Ac-modified cells than the cells treated with and without natural CMP-Neu5Ac, respectively. ^{BPC}Neu5Ac and ^{MPB}Neu5Ac installed on the cell surface in the α 2-3-linkage only exhibited very weak CD22-Fc binding on Lec2 cells (Figure 2c and Supplementary figure s6c) and HEK293- ST cells (Supplementary figure s6e and s6f). Notably, under saturating conditions approximately 2fold higher CD22-Fc binding was detected on **2a** and **2b** modified HEK293- ST cells than their Lec2 counterparts, respectively, (Figure 2d). This observation suggests that cell-specific glycan scaffolds may influence binding to CD22 ligands engineered on the surface.

Engineering high-affinity ligands on NK-92MI and CIK cells for efficient CD22-targeting.

After confirming that **2a** and **2b** can be incorporated onto mammalian cell surfaces via ST6Gal1-mediated sialylation to create high-affinity CD22 ligands, we then explored the

feasibility of using this strategy to engineer NK-92MI and CIK cells for targeting tumor cells expressing CD22. To prepare CIK cells, peripheral blood mononuclear cells from healthy donors were activated with anti-CD3 and anti-CD28 antibodies, and maintained in IL-2 supplemented T-cell culture medium for 10–15 days.^[26] After subjecting NK-92MI and CIK cells to ST6Gal1-mediated sialylation, both cell lines exhibited dramatically enhanced binding to CD22-Fc in a dose- and time-dependent manner (Figure 2e, 2g, Supplementary figure s7a, and s8a). Under saturating concentrations of CMP-^{BPC}Neu5Ac and CMP-^{MPB}Neu5Ac, the high affinity ligand modified NK-92MI cells showed approximately 20–50-fold higher CD22 binding in comparisons to their counterparts treated with CMP-Neu5Ac to install the natural ligands. Likewise, CMP-^{BPC}Neu5Ac- and CMP-^{MPB}Neu5Ac-modified CIK cells showed approximately 10fold higher CD22 binding compared to their counterparts treated with CMP-Neu5Ac. As expected, ST6Gal1-mediated sialylation significantly increased the abundance of the bi-antennary, tri-antennary, and created several new sialosides on NK-92MI cells (Supplementary figure s9). We also confirmed that the newly created CD22 ligands did not impair the proliferation and cell viability of NK-92MI and CIK cells (Supplementary figure s7c-e, and s8c). Three days after *in vitro* sialylation, even with proliferation- or turnover-associated dilution of cell-surface ligands the modified NK-92MI and CIK cells still showed approximately 10 and 15 fold better CD22-Fc binding than the untreated cells, respectively (Supplementary figure s7f and s8b). Desialylation by neuraminidase treatment followed by enzymatic sialylation of NK-92MI and CIK cells did not increase CD22 binding (Figure 2f, Supplementary figure s7b, s8h and s8i), but rather impaired CD22 binding especially when the natural donor substrate CMP-Neu5Ac was used for sialylation. This observation suggests that in the natural scenario, Neu5Ac α 2-6Gal β 1-4GlcNAc on *O*-glycans and glycolipid also contribute significantly toward CD22 binding. However, when the high-affinity CD22 ligands are incorporated onto *N*-glycans, the contributions of the natural ligands on *O*-glycans and glycolipid become less important.

Killer cells armed with CD22-ligands exhibit significantly enhanced binding and killing of B-lymphoma cells in vitro.

Enhanced CD22-Fc binding of the ligand functionalized NK-92MI and CIK cells should translate into their enhanced ability to induce the binding and killing of tumor cells with CD22 overexpression. The targeting efficiency of CD22-ligand-functionalized NK-92MI and CIK for B-lymphoma cells with high CD22 expression was assessed by quantifying the formation of cell-cell conjugates when coculturing NK-92MI or CIK (effector cells, E) and B-lymphoma cells (target cells, T). In comparison to the unmodified counterparts, the CD22-ligand modified NK-92MI and CIK significantly increased the formation of cell-cell conjugates, respectively. The higher the level of CD22 expression of target cells (Figure 3a), the higher percentage of conjugate formation was detected (Figure 3b, 3c, Supplementary figure s8d, s8e, and s10). Modified Killer cells did not induce enhanced cluster formation with Jurkat cells that are CD22 negative. Consistent with the enhanced binding, the functionalized NK-92MI and CIK cells induced better killing of target B-lymphoma cells (Figure 3d-h, Supplementary figure s8f, and s8g), which was further supported by the increased IFN-gamma production (Supplementary figure s11).

Next, we tested CD22-targeting efficiency in the presence of red blood cells (RBCs) to better mimic the *in vivo* scenario. RBC present nature ligands of CD22 on their cell surface as revealed by CD22-Fc staining (Supplementary figure s12). Interestingly, CD22-ligand-mediated targeting of NK-92MI and CIK cells to B-lymphoma cells was 2fold improved after docking 100 times of RBC cells into the co-culture systems (Figure 3i, 3j and Supplementary figure s8d). As expected, human RBCs functionalized with high-affinity CD22 ligands did not induce the killing of Raji and Daudi cells (Supplementary figure s13). Importantly, while the modified NK-92MI cells bound to normal B cells from healthy donors, there was no apparent specific lysis detected (Figure 3a and Supplementary figure s14). Together, these results suggest that killer cells armed with CD22-ligands may be a biocompatible tool for selective eradication of B-lymphoma.

Exploiting glycan engineering for efficient NK-92MI-immunotherapy in a mouse model.

The antitumor efficacies of NK-92MI armed with high-affinity CD22 ligands were next evaluated *in vivo* using a xenograft model. Raji cells expressing firefly luciferase (Raji-Luc) were intravenously (*i.v.*) administered into NSG mice on day 0, followed by three NK-92MI injections (*i.v.*) on day 2, day 6, and day 10. Tumor growth was monitored by longitudinal, non-invasive bioluminescence imaging (Figure 4a and 4b). Compared to the control group that received buffer injection only, no significant inhibition of Raji-Luc tumor growth was observed in the group treated with unmodified NK-92MI cells, whereas ^{BPC}Neu5Ac-NK-92MI cells exhibited moderate capabilities to suppress tumor growth with ~25% reduction in bioluminescence signals relative to the control group treated with the buffer only (Figure 4b). Although we only observed relatively weak reduction in the tumor associated bioluminescence signals, adoptive transfer of ^{BPC}Neu5Ac-NK-92MI cells did confer the recipient mice with pronounced survival benefit. In the control group that received buffer injection only and the group that received unfunctionalized NK-92MI cells, mouse death started to be observed on day 15 and no mice survived to day 19. By contrast, in the group that received ^{BPC}Neu5Ac-NK-92MI cells, mice started to die on day 17 and by day 19 there were still 5 mice alive.

Because most leukemia and lymphoma cells require a close relationship with the bone marrow microenvironment for their survival and disease progression.^[39,40] The low efficacy of ^{BPC}Neu5Ac-NK-92MI cells *in vivo* suggest that the modified NK cells may not be sufficiently trafficking to bone marrow to attack B lymphoma where they reside *in situ*. The cell adhesion molecule E-selectin is constitutively expressed in the bone marrow and plays a critical role in promoting leukemia cell adhesion, survival, and resistance to chemotherapy.^[41] Consistent with this knowledge, we noticed that upon *i.v.* injection, the injected Raji-Luc cells primarily migrated to the bone marrow and the circulating Raji-Luc cells was only detectable in the bloodstream until late stages (i.e. 14-16 days after Raji inoculation). By contrast, the majority of the injected NK-92MI cells were found in the lung, spleen and blood steam.^[19,27] Based on this observation, we hypothesized that increasing bone marrow infiltration would increase NK-induced tumor cell targeting and killing. The rolling and tethering of leukocytes on inflamed vessel endothelium cells rely on the binding of cell-surface sialyl Lewis X (sLe^X, Neu5Acα2-3Galβ1-4(Fuca1-3)GlcNAc) with E-selectin to initialize tissue entry from the bloodstream, and importantly, cells migrate to bone through

specialized marrow vessels that constitutively express vascular E-selectin. Therefore, we explored the possibility of creating sLe^X on the NK-92MI surface to enhance their interactions with E-selectin and thus facilitate bone migration.^[42] The similar strategy was employed previously by Sackstein and coworker to tune human multipotent mesenchymal stromal cell (MSC) trafficking to bone.^[43]

To create sLe^X on NK-92MI, the cells were treated with human fucosyltransferase 6 (FUT6)^[33,43-45] and GDP-fucose. The successful fucosylation and creation of sLe^X on NK-92MI cells were respectively confirmed by *Aleuria aurantia* lectin (AAL, specific for α 1-3- and α 1-6-linked fucose) and sLe^X-specific antibody staining (Figure 4c). The PNGase F-mediated *N*-glycan cleavage partially removed the newly added fucose, suggesting that fucose residues were added to both *N*- and *O*-glycans (Supplementary figure s14a). The dual-modified NK-92MI cells that display both sLe^X and CD22 ligands exhibited comparable Raji killing capabilities as ^{BPC}Neu5Ac-NK-92MI cells (Figure 4d). Next, proteomics analysis was performed to profile the membrane glycoproteins modified by fucosylation using biotinylated GDP-fucose as the donor substrate, through which 119 proteins were identified with high confidence (spectra count number 5 proteins were listed in Supplementary table 1). Besides CD44 that was discovered previously to be crucial for bone marrow migration of MSC,^[44] other proteins that were also α 1-3-fucosylated including integrins, neural cell adhesion molecule (NCAM1), fibronectin 1 (FN1), human leukocyte antigen (HLA) and CD48 *etc.* (Supplementary figure s14). To further assess if the newly created sLe^X promoted NK-92MI bone migration, dual-functionalized or ^{BPC}Neu5Ac-modified NK-92MI cells were injected (*i.v.*) into NSG mice that had been inoculated with Raji-Luc for 12 day. The NK-92MI subsets in the periphery blood and the hind-leg bone marrow were quantified 10 hours later (Figure 4e). Compared to ^{BPC}Neu5Ac-NK-92MI cells without FUT6-treatment, the bone marrow colonization of (^{BPC}Neu5Ac)-sLe^X-NK-92MI increased approximately 60% with a concomitant decrease of circling (^{BPC}Neu5Ac)-sLe^X-NK-92MI in the blood stream.

In contrast to the NK-92MI cells modified with CD22-ligand alone, these dual-functionalized NK-92MI cells showed remarkably enhanced capabilities to control Raji cell growth compared to ^{BPC}Neu5Ac-NK-92MI (Figure 4a, 4b, 4f, and 4g). The lifespan of tumor-bearing NSG mice was extended approximately 27% in the (^{BPC}Neu5Ac)-NK-92MI cell treated group and 40% in (^{BPC}Neu5Ac)-sLe^X-NK-92MI cell treated group, respectively, compared to the control group treated with buffer only. Since NK-92MI cells are well documented not to effectively kill tumor cells unless they are endowed with tumor targeting capabilities,^[21,22] and we have shown that sLe^X modification does not increase NK-92 cell killing, we conclude that these doubly modified cells are likely effective as a result of CD22 ligands enabling engagement of CD22 on Raji cells, and that sLe^X more effectively targets the NK cells to protective tumor microenvironments like the bone marrow.

Conclusion and Discussion

Molecules presented on the cell surface determine how cells interact with their partners and their environment. By engineering the cell-surface landscape, cells can be endowed with the desired properties. In our previous studies^[46], by exploiting the donor substrate promiscuity

of *H. pylori* fucosyltransferase, we demonstrated that HER2-specific antibody Herceptin were efficiently installed onto the cell-surface of NK-92MI cells. The resulting Herceptin-NK-92MI conjugates exhibited remarkably enhanced activities to induce the lysis of HER2-positive cancer cells both *ex vivo* and in a human tumor xenograft model. In the current study, we utilized ST6Gal1-mediated sialylation to create high-affinity CD22 ligands directly on NK-92MI cells. Via this approach significantly higher levels of CD22 ligands could be installed onto the cell surface in comparison to metabolic oligosaccharide engineering (MOE)-based ligand incorporation conducted by the Huang group^[46] (Supplementary figure s16). It is apparent that there is sufficiently high level of endogenous un-sialylated LacNAc residues that can be readily modified by ST6Gal1 to create a significant level of CD22 ligands. By contrast, the unnatural sialic acids (e.g., **1a** and **1b**) when added to the culture media for incorporation through the metabolic pathway can be inefficient as a result of competing with the natural sialic acid (Neu5Ac) for *de novo* sialylation of glycoproteins.

Major efforts on cancer immunotherapy are focused on the discovery of new tumor-specific antigens and ways to target them specifically. Relatively less attention has been devoted to approaches to facilitate the trafficking and tumor infiltration of immune cells. In their pioneering work, Sackstein, Xia et al., applied chemoenzymatic glycan editing based on human α 1-3-fucosyltransferase (FUT) to create sLe^X on human multipotent mesenchymal stromal cells^[44] and cord blood cells^[43] so as to enhance their engraftment and trafficking. Although a previous study introducing CD22 ligands into NK cells resulted in NK cell killing of B lymphoma cells as shown here,^[47] we found that equipping NK-92MI cells with selectin ligands in addition to CD22 ligands enhanced their efficacy in a B cell lymphoma model, where Raji B-lymphoma cells are localize in the bone marrow. For this reason, we suggest that the efficient trafficking of NK-92MI cells to bone marrow via engineered selectin ligands is critical for inducing productive tumor control.

In summary, cell-surface chemoenzymatic glycan editing offers an easy-to-practice strategy to boost the efficacy of therapeutic cells for better cancer treatment. Despite glycan turn-over and cell proliferation, a significant portion of CD22 ligands still remain on the cell surface after 72 hrs, which is in line with the persistence time of irradiated NK-92MI cells in human patients. Therefore, this technique provides a nice complement or synergistic approach to the permanent, genetic engineering approach that has found great success in constructing NK-92MI-based CAR-NK cells.

Experimental Section

Assessment of the NK-92MI cytotoxicity against B-lymphoma cells and CD22-negative Jurkat cells:

Labeled or unlabeled NK-92MI cells were co-cultured with different types of cancer cells at the indicated effector/target ratios for 4 hours in a 96-well plate. Specific cancer cell lysis was detected by LDH secretion in supernatant (CytoTox96, Promega). Setup of control groups and calculations of specific lysis were done according to the manufacturer's instructions. The supernatant of each group (1-hour incubation) was also collected and subjected to IFN-gamma ELISA kits for quantification.

NSG mice model for assessing NK-92MI based killing of CD22-positive B-lymphoma cells:

Male NSG mice (8-12 weeks old) were inoculated with 1×10^6 Raji-Luc cells through tail vein injection (day 0). On day 2, mice were randomly divided into four groups and treated with HBSS, NK-92MI, BPC Neu5Ac-modified NK-92MI, or BPC Neu5Ac/sLe^X dual-labeled NK-92MI cells through tail vein injection (10×10^6 NK-92MI cells per mouse). On day 5 after tumor challenge, mice were injected with 200 μ L D-luciferin (15 mg/mL) through *i.p.* injection. After 10 minutes, the bioluminescence signal in the mice was analyzed by the PerkinElmer IVIS system. The total photons indicating the tumor were quantified by the IVIS software. For tracing B-lymphoma progression, the NSG mice further received two additional NK-92MI doses on days 6 and 10. The luciferin-assisted IVIS monitoring of tumor growth were performed on day 5, day 7, day 12, and day 15. For the established tumor model, NSG mice were injected intravenously with 1×10^6 Raji-Luc cells on day 0. The animals were imaged to confirm B-lymphoma formation and received one treatment of 10×10^6 NK-92MI or sLe^X-NK-92MI cells (*i.v.* injection) on day 12.

Supplementary Material

Refer to Web version on PubMed Central for supplementary material.

Acknowledgements

Financial support was from the NIH (R01GM093282, R01GM113046 and R01AI143884 to P.W., P41GM103390, P01GM107012, and R01GM130915 to K.W.M., R01AI050143, P01HL107151, and U19AI136443 to J.C.P.), and from the Danish National Research Foundation (DNRF107 to H.C. and Y.N.)

References

- [1]. Smith MR Rituximab (monoclonal anti-CD20 antibody): mechanisms of action and resistance. *Oncogene* 2003, 22, 7359–7368. [PubMed: 14576843]
- [2]. Marshall MJE, Stopforth RJ & Cragg MS Therapeutic Antibodies: What Have We Learnt from Targeting CD20 and Where Are We Going? *Front Immunol* 2017, 8, 1245. [PubMed: 29046676]
- [3]. Müller J & Nitschke L The role of CD22 and Siglec-G in B-cell tolerance and autoimmune disease. *Nat. Rev. Rheumatol* 2014, 10, 422–428. [PubMed: 24763061]
- [4]. Macauley MS, Crocker PR & Paulson JC Siglec-mediated regulation of immune cell function in disease. *Nat. Rev. Immunol* 2014, 14, 653–666. [PubMed: 25234143]
- [5]. Mullard A Maturing antibody-drug conjugate pipeline hits 30. *Nat Rev Drug Discov* 2013, 12, 329–332. [PubMed: 23629491]
- [6]. Ramakrishna S et al. Modulation of Target Antigen Density Improves CAR T-cell Functionality and Persistence. *Clin. Cancer Res* 2019, 25, 5329–5341. [PubMed: 31110075]
- [7]. Fry TJ et al. CD22-targeted CAR T cells induce remission in B-ALL that is naive or resistant to CD19-targeted CAR immunotherapy. *Nat. Med* 2018, 24, 20–28. [PubMed: 29155426]
- [8]. Lee DW et al. T cells expressing CD19 chimeric antigen receptors for acute lymphoblastic leukaemia in children and young adults: a phase 1 dose-escalation trial. *Lancet* 2015, 385, 517–528. [PubMed: 25319501]
- [9]. Rosenberg SA & Restifo NP Adoptive cell transfer as personalized immunotherapy for human cancer. *Science* 2015, 348, 62–68. [PubMed: 25838374]
- [10]. Kelm S, Gerlach J, Brossmer R, Danzer CP & Nitschke L The ligand-binding domain of CD22 is needed for inhibition of the B cell receptor signal, as demonstrated by a novel human CD22-specific inhibitor compound. *J. Exp. Med* 2002, 195, 1207–1213. [PubMed: 11994426]

- [11]. Kelm S et al. C-4 modified sialosides enhance binding to Siglec-2 (CD22): towards potent Siglec inhibitors for immunoglycotherapy. *Angew. Chem. Int. Ed. Engl* 2013, 52, 3616–3620. [PubMed: 23440868]
- [12]. Rillahan CD et al. On-chip synthesis and screening of a sialoside library yields a high affinity ligand for Siglec-7. *ACS Chem. Biol* 2013, 8, 1417–1422. [PubMed: 23597400]
- [13]. Büll C, Heise T, Adema GJ & Boltje TJ Sialic Acid Mimetics to Target the Sialic Acid-Siglec Axis. *Trends Biochem. Sci* 2016, 41, 519–531. [PubMed: 27085506]
- [14]. Peng W & Paulson JC CD22 Ligands on a Natural N-Glycan Scaffold Efficiently Deliver Toxins to B-Lymphoma Cells. *J. Am. Chem. Soc* 2017, 139, 12450–12458. [PubMed: 28829594]
- [15]. Chen WC et al. In vivo targeting of B-cell lymphoma with glycan ligands of CD22. *Blood* 2010, 115, 4778–4786. [PubMed: 20181615]
- [16]. Bednar KJ et al. Human CD22 Inhibits Murine B Cell Receptor Activation in a Human CD22 Transgenic Mouse Model. *J. Immunol* 2017, 199, 3116–3128. [PubMed: 28972089]
- [17]. Orgel KA et al. Exploiting CD22 on antigen-specific B cells to prevent allergy to the major peanut allergen Ara h 2. *J. Allergy Clin. Immunol* 2017, 139, 366–369.e2. [PubMed: 27554819]
- [18]. Suck G et al. NK-92: an ‘off-the-shelf therapeutic’ for adoptive natural killer cell-based cancer immunotherapy. *Cancer Immunol. Immunother* 2016, 65, 485–492. [PubMed: 26559813]
- [19]. Zhu L et al. Natural Killer Cell (NK-92MI)-Based Therapy for Pulmonary Metastasis of Anaplastic Thyroid Cancer in a Nude Mouse Model. *Front. Immunol* 2017, 8, 816. [PubMed: 28785259]
- [20]. Klingemann H, Boissel L & Toneguzzo F Natural Killer Cells for Immunotherapy - Advantages of the NK-92 Cell Line over Blood NK Cells. *Front. Immunol* 2016, 7, 91. [PubMed: 27014270]
- [21]. Zhang C et al. ErbB2/HER2-Specific NK Cells for Targeted Therapy of Glioblastoma. *J. Natl. Cancer Inst* 2016, 5, djv375.
- [22]. Zhang C et al. Chimeric Antigen Receptor-Engineered NK-92 Cells: An Off-the-Shelf Cellular Therapeutic for Targeted Elimination of Cancer Cells and Induction of Protective Antitumor Immunity. *Front. Immunol* 2017, 8, 533. [PubMed: 28572802]
- [23]. Kim HM et al. Anti-tumor activity of ex vivo expanded cytokine-induced killer cells against human hepatocellular carcinoma. *Int. Immunopharmacol* 2007, 7, 1793–1801. [PubMed: 17996690]
- [24]. Sangiolo D et al. Cytokine-induced killer cells eradicate bone and soft-tissue sarcomas. *Cancer Res.* 2014, 74, 119–129. [PubMed: 24356422]
- [25]. Wei F et al. Cytokine-induced killer cells efficiently kill stem-like cancer cells of nasopharyngeal carcinoma via the NKG2D-ligands recognition. *Oncotarget* 2015, 6, 35023–35039. [PubMed: 26418951]
- [26]. Lee JH et al. Sustained efficacy of adjuvant immunotherapy with cytokine-induced killer cells for hepatocellular carcinoma: an extended 5-year follow-up. *Cancer Immunol. Immunother* 2019, 68, 23–32. [PubMed: 30232520]
- [27]. Pittari G, Filippini P, Gentilcore G, Grivel JC & Rutella S Revving up Natural Killer Cells and Cytokine-Induced Killer Cells Against Hematological Malignancies. *Front Immunol.* 2015, 6, 230. [PubMed: 26029215]
- [28]. Macauley MS & Paulson JC Immunology: glyco-engineering ‘super-self’. *Nat. Chem. Biol* 2016, 10, 7–8.
- [29]. López-Aguilar A et al. Tools for Studying Glycans: Recent Advances in Chemoenzymatic Glycan Labeling. *ACS Chem. Biol* 2017, 12, 611–621. [PubMed: 28301937]
- [30]. Rillahan CD, Schwartz E, McBride R, Fokin VV & Paulson JC Click and pick: identification of sialoside analogues for siglec-based cell targeting. *Angew. Chem. Int. Ed. Engl* 2012, 51, 11014–11018. [PubMed: 23038623]
- [31]. Li Y, Yu H, Cao H, Muthana S & Chen X Pasteurella multocida CMP-sialic acid synthetase and mutants of Neisseria meningitidis CMP-sialic acid synthetase with improved substrate promiscuity. *Appl. Microbiol. Biotechnol* 2012, 93, 2411–2423. [PubMed: 21968653]
- [32]. Narimatsu Y et al. An Atlas of Human Glycosylation Pathways Enables Display of the Human Glycome by Gene Engineered Cells. *Mol. Cell* 2019, 75, 394–407.e5. [PubMed: 31227230]

- [33]. Moremen KW et al. Expression system for structural and functional studies of human glycosylation enzymes. *Nat. Chem. Biol* 2018, 14, 156–162. [PubMed: 29251719]
- [34]. Nycholat CM et al. Synthesis of biologically active N- and O-linked glycans with multisialylated poly-N-acetylglucosamine extensions using *P. damsela* α 2-6 sialyltransferase. *J. Am. Chem. Soc* 2013, 135, 18280–18283. [PubMed: 24256304]
- [35]. Kajihara Y et al. A Novel α -2,6-Sialyltransferase: Transfer of Sialic Acid to Fucosyl and Sialyl Trisaccharides. *J. Org. Chem* 1996, 61 8632–8635.
- [36]. Hong S et al. Bacterial glycosyltransferase-mediated cell-surface chemoenzymatic glycan modification. *Nat. Commun* 2019, 10, 1799. [PubMed: 30996301]
- [37]. Siegler EL, Zhu Y, Wang P & Yang L Off-the-Shelf CAR-NK Cells for Cancer Immunotherapy. *Cell Stem Cell* 2018, 23, 160–161. [PubMed: 30075127]
- [38]. Williams BA et al. A phase I trial of NK-92 cells for refractory hematological malignancies relapsing after autologous hematopoietic cell transplantation shows safety and evidence of efficacy. *Oncotarget* 2017, 8, 89256–89268. [PubMed: 29179517]
- [39]. Winkler IG et al. Vascular E-Selectin Protects Leukemia Cells from Chemotherapy By Directly Activating Pro-Survival NF-Kb Signalling - Therapeutic Blockade of E-Selectin Dampens NF-Kb Activation. *Blood* 2016, 128, 2823–2823.
- [40]. Spertini C et al. Acute Myeloid and Lymphoblastic Leukemia Cell Interactions with Endothelial Selectins: Critical Role of PSGL-1, CD44 and CD43. *Cancers (Basel)* 2019, 11,1253 .
- [41]. Sircar A et al. Impact and Intricacies of Bone Marrow Microenvironment in B-cell Lymphomas: From Biology to Therapy. *Int. J. Mol. Sci* 2020, 21, 904.
- [42]. Phillips ML et al. ELAM-1 mediates cell adhesion by recognition of a carbohydrate ligand, sialyl-Lex. *Science* 1990, 250, 1130–1132. [PubMed: 1701274]
- [43]. Xia L et al. Surface fucosylation of human cord blood cells augments binding to P-selectin and E-selectin and enhances engraftment in bone marrow. *Blood* 2004, 104, 3091–3096. [PubMed: 15280192]
- [44]. Sackstein R et al. Ex vivo glycan engineering of CD44 programs human multipotent mesenchymal stromal cell trafficking to bone. *Nat. Med* 2008, 14, 181–187. [PubMed: 18193058]
- [45]. Mondal N, Silva M, Castano AP, Maus MV & Sackstein R Glycoengineering of chimeric antigen receptor (CAR) T-cells to enforce E-selectin binding. *J. Biol. Chem* 2019, 294, 18465–18474. [PubMed: 31628196]
- [46]. Li J et al. A Single-Step Chemoenzymatic Reaction for the Construction of Antibody-Cell Conjugates. *ACS Cent. Sci* 2018, 4, 1633–1641. [PubMed: 30648147]
- [47]. Wang X et al. Glycoengineering of Natural Killer Cells with CD22 Ligands for Enhanced Anticancer Immunotherapy. *ACS Cent. Sci* 2020, 6, 382–389. [PubMed: 32232138]

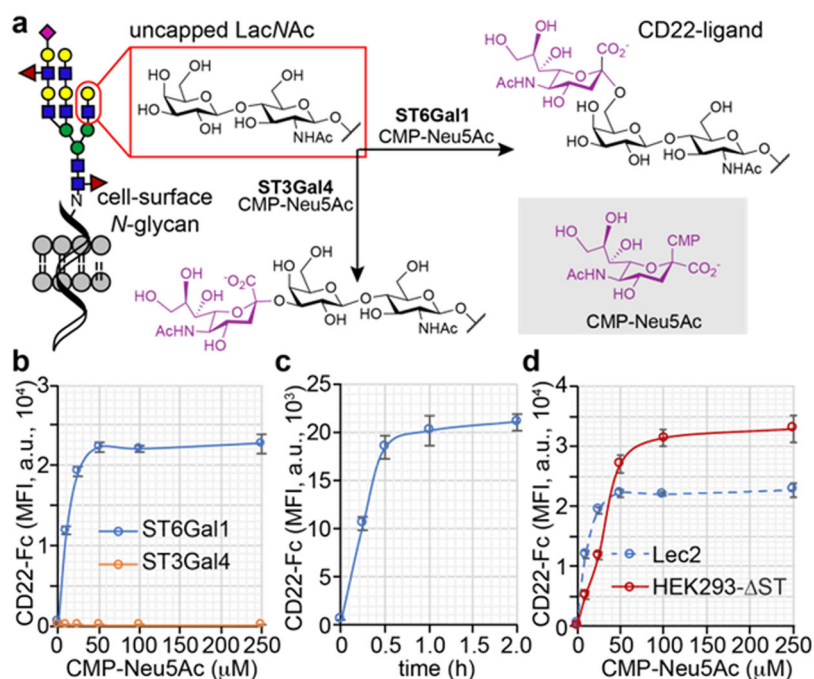
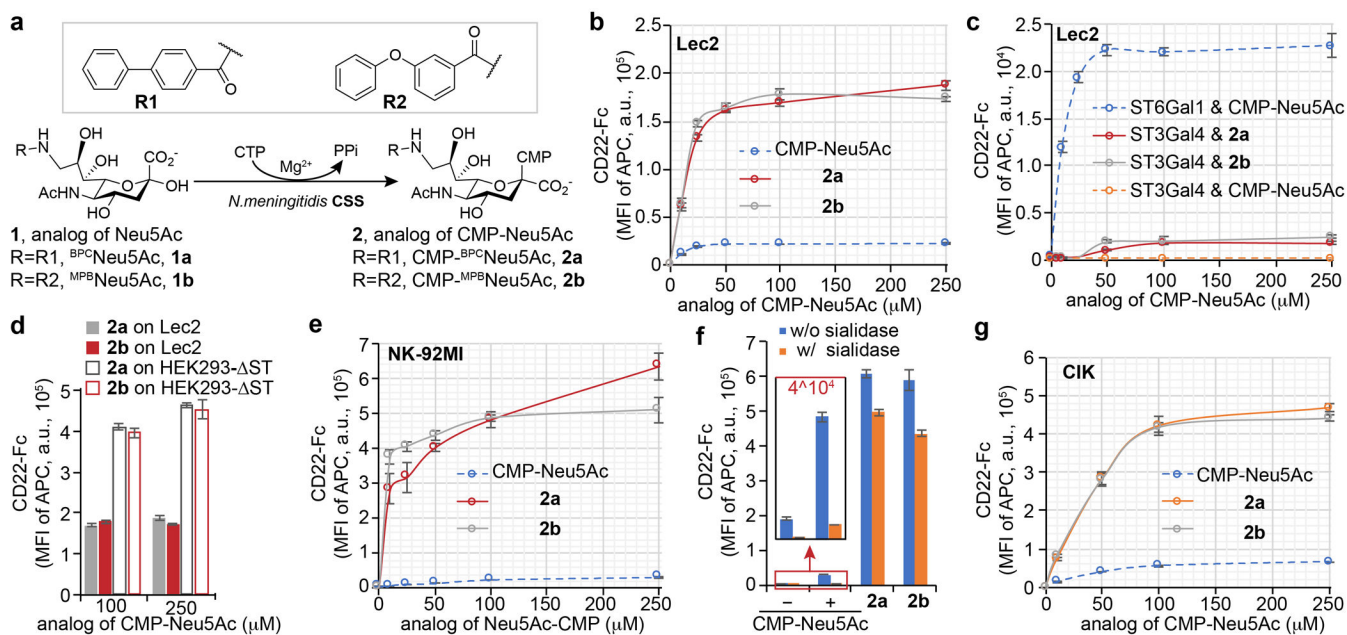
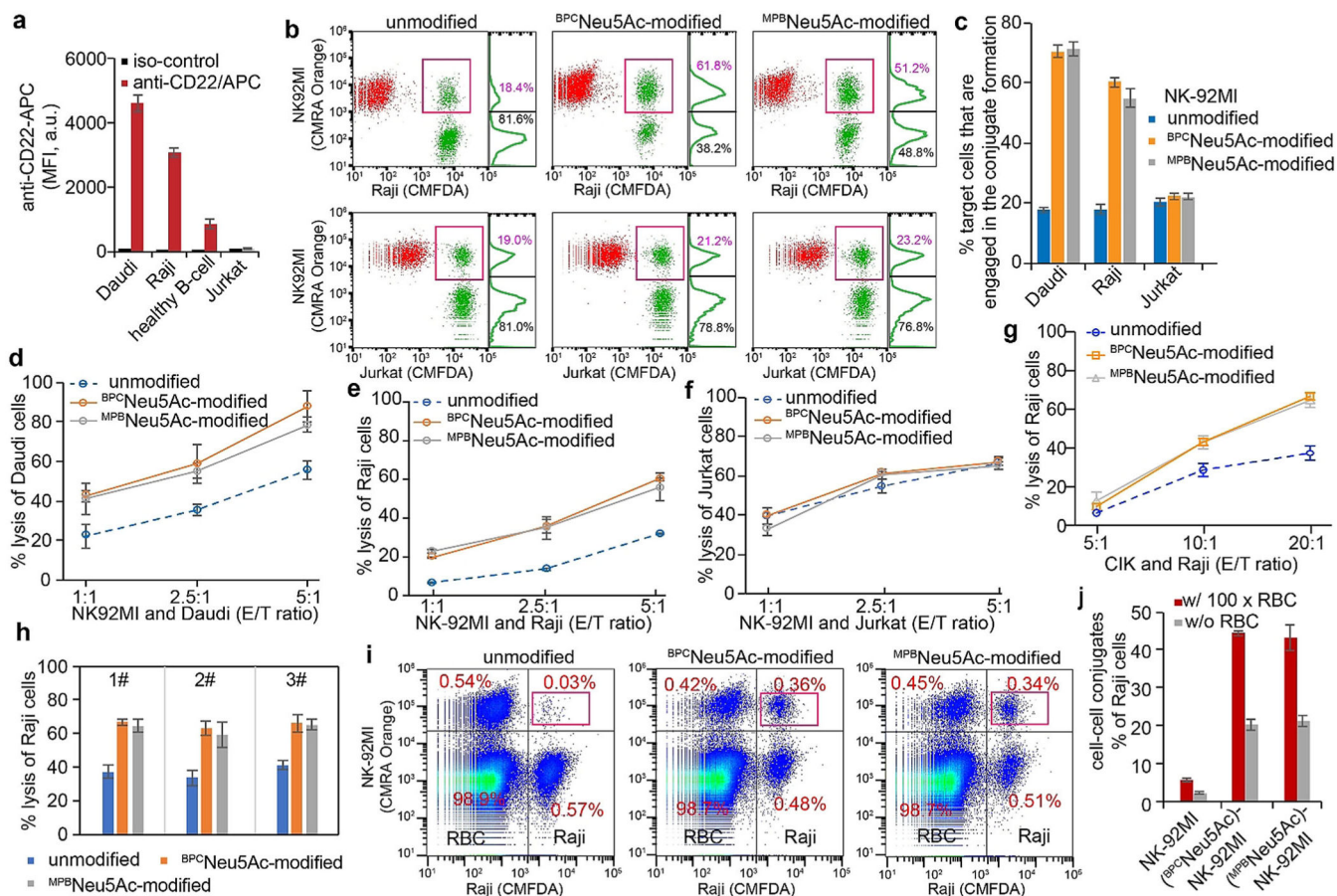


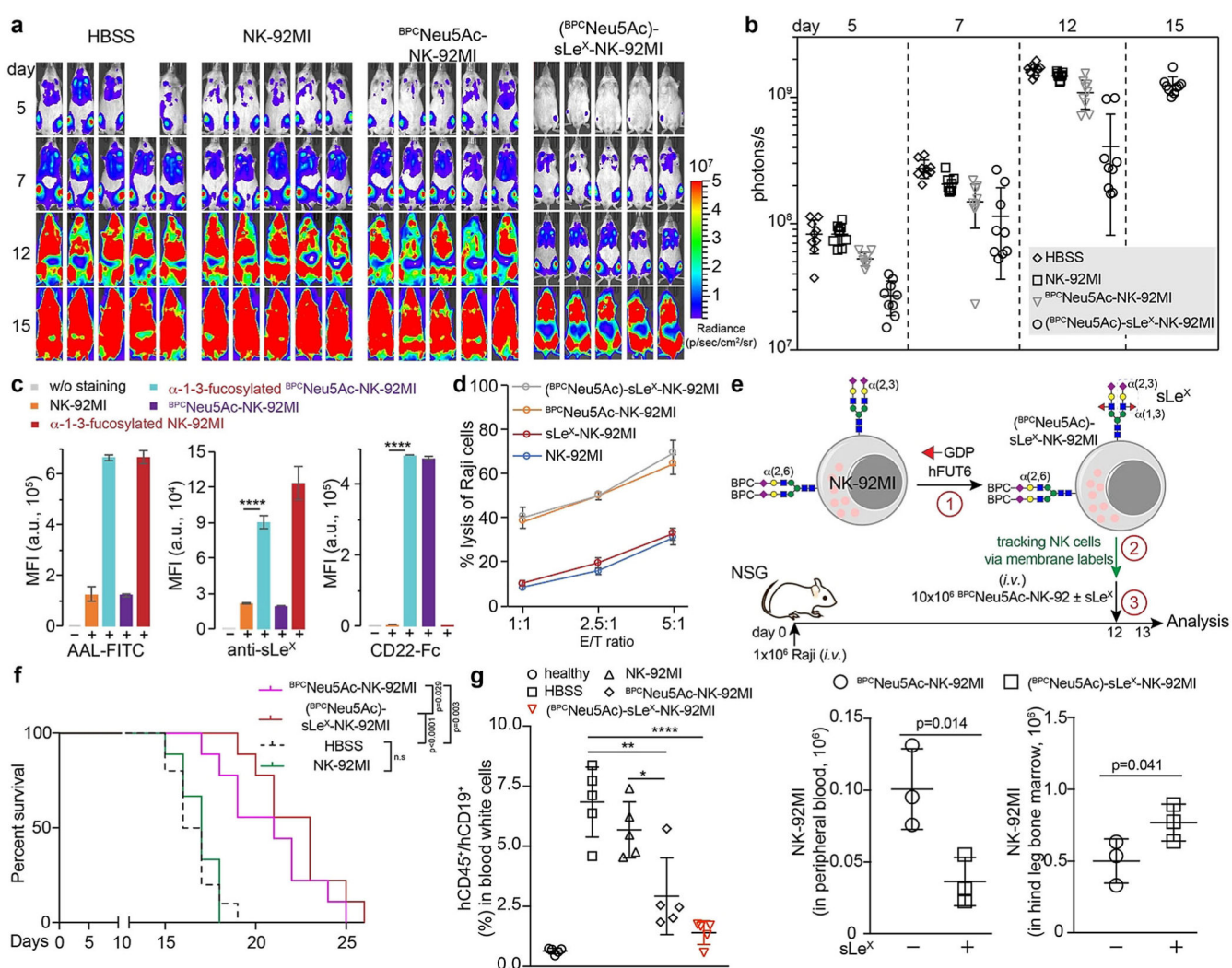
Figure 1. Chemo-enzymatic generation of sialyl ligands on live cells to increase CD22 binding. (a) ST6Gal1- and ST3Gal4-assisted incorporation of Neu5Ac onto type 2 LacNAc in α 2-6- and α 2-3-linkages, respectively. The resulting Neu5Ac α 2-6Gal β 1-4GlcNAc is a natural ligand of CD22, whereas Neu5Ac α 2-3Gal β 1-4GlcNAc is not. (b-d) Flow cytometry quantification of CD22-Fc binding of ST-engineered live cells. The error bars represent the standard deviation of three biological replicates. (b) Creation of CD22 ligands on Lec2 cells by STs-mediated glycan editing was assessed with CD22-Fc. (c) Using CD22-Fc to probe time-dependent creation of CD22 ligands on Lec2 cells by ST6Gal1-mediated glycan editing. (d) Comparison of CD22-Fc binding of Lec2 and HEK293- ST mutant cells modified by ST6Gal1.

**Figure 2.**

hSTs-assisted creation of high-affinity CD22-ligands on live cells. (a) synthesis of C-9 functionalized analogs of CMP-Neu5Ac, including CMP^{BPC}Neu5Ac (**2a**) and CMP^{BPC}Neu5Ac (**2b**). (b-g) flow cytometry quantification of CD22-Fc binding onto STs-engineered live cells, including Lec2, HEK293- ST, NK-92MI and CIK cells. The error bars represent the standard deviation of three biological replicates. The CD22-Fc based probing of the ST6Gal1- (b) or ST3Gal4-assisted (c) incorporation of unnatural sialic acids (**2a** or **2b**) or nature sialic acid (Neu5Ac) onto Lec2 cells. (d) Comparison of CD22-Fc binding of Lec2 and HEK293- ST mutant cells modified by ST6Gal1 and unnatural CMP sialic acids. (e and f) The newly created CD22 ligands on NK-92MI cells were probed with CD22-Fc, after incubation with ST6Gal1 and the indicated substrates of different concentrations. (e) or NK-92MI cells pretreated by sialidase or not (f). (g) The CD22-Fc based probing of the ST6Gal1-assisted incorporation of sialic acids onto CIK cells.

**Figure 3.**

Targeting B-lymphoma with the CD22-sialoside-ligands armed killer cells. (a) Comparison of CD22 expression levels on different types of cells, including two B-lymphoma cell lines Daudi and Raji, B-cell from six healthy donors, as well as the T-lymphoma cell line Jurkat. (b and c) Flow cytometry-based detection of cell-cell conjugates of NK-92MI cells (effector cell, stained with CMRA Orange) and target cells (Raji or Jurkat cells, stained with CMFDA Green) at an E/T ratio of 5:1. Number (in purple) indicates the ratio of target cells (i.e., Raji or Jurkat cells) that form clusters with NK-92MI cells. (c) The relative proportion of NK-92MI cell-target cell conjugates with target cells. (d-h) LDH release assay based quantifying of killer cell cytotoxicity against Daudi (d), Raji (e, g and h), and Jurkat cells (f). In figure d-f, NK-92MI was the effector cell. In figure g and h, CIK was the effector cell. (i and j) Flow cytometry-based detection of cell-cell conjugate formation of NK-92MI cells and Raji cells (E/T ratio, 1:1), after docking of 100 × excess human red blood cells (RBC) or not.

**Figure 4.**

Suppression of Raji B-lymphoma proliferation by the functionalized NK-92MI cells in a murine xenograft model. The B-lymphoma xenograft was established by tail vein injection of 1 million Raji-Luc cells into NSG mice on day 0. On day 2, the tumor-bearing mice received the 1st treatment by i.v. infusion of 10 million NK-92MI cells, NK-92MI cells conjugated with $BPCNeu5Ac$ ($BPCNeu5Ac$ -NK-92MI), and $(BPCNeu5Ac)$ -sLe^X-NK-92MI, respectively; control groups received a single injection of the vehicle (HBSS). The 2nd and 3rd NK-92MI cell infusions were performed on day 6 and 10, respectively (a and b). On days 5, 7, 12, and 15, the mice were i.p. injected with D-luciferin and imaged by the IVIS system. (c) FUT6-assisted creation of sLe^X on NK-92MI cells. $BPCNeu5Ac$ was conjugated to NK-92MI by ST6Gal1, which was followed by FUT6-assisted α 1-3-fucosylation to create the sLe^X epitope. The cell-surface creation of α 1-3-fucosides, sLe^X and CD22-ligands was confirmed by AAL lectin (left), anti-sLe^X antibody (middle), and CD22-Fc staining (right). (d) Quantify NK-mediated Raji cell killing using a LDH release assay. In figure c and d, the error bars represent the standard deviation of three biological replicates. (e) The workflow for the adoptive transfer of $BPCNeu5Ac$ -NK-92MI cells with or without sLe^X addition to

tumor-bearing NSG mice. After overnight circulation, the peripheral blood and bone marrow localization of NK cells were analyzed by flow cytometry. p values were calculated via a two-sided Student's t-test. (f) Survival of mice after NK-92MI cell therapy illustrated by Kaplan-Meier curves. Shown are nine mice per treatment group pooled from three independent experiments. P values are calculated via Log-Rank (Mantel-Cox) test. (g) On day 16, the blood of tumor-bearing mice was collected, and the Raji cells (CD19⁺) in blood samples were analyzed with flow cytometry. * indicates the two-sided Students' t-test $p < 0.05$, ** indicates the two-sided Students' t-test $p < 0.01$, **** indicates the two-sided Students' t-test $p < 0.001$.

Author Manuscript

Author Manuscript

Author Manuscript

Author Manuscript